

Electrochemical DNA Sensor for *hly* Gene of *Listeria Monocytogenes* by Three-Dimensional Graphene and Gold Nanocomposite Modified Electrode

Lijun Yan, Wenshu Zhao, Zuorui Wen, Xiaoyan Li, Xueliang Niu, Yaqi Huang, Wei Sun*

Key Laboratory of Tropical Medicinal Plant Chemistry of Ministry of Education, College of Chemistry and Chemical Engineering, Hainan Normal University, Haikou 571158, P. R. China

*E-mail: swyy26@hotmail.com

Received: 25 January 2017 / Accepted: 6 March 2017 / Published: 12 April 2017

A high performance electrochemical DNA sensor with three-dimensional graphene (3DGR) and gold (Au) nanocomposite modified electrode was developed for sensitive analysis of specific *hly* gene of *Listeria monocytogenes*. Nanocomposite was synthesized by electrochemical deposition of 3DGR and Au in turn on carbon ionic liquid electrode (CILE). Mercaptoacetic acid (MAA) was self-assembled on Au/3DGR/CILE by the specific binding of Au-S bond, which was used for the covalently linkage of ssDNA probe sequences. The fabricated ssDNA/MAA/Au/3DGR/CILE could interact with the target ssDNA sequence and the hybridization was recorded by using electrochemical indicator methylene blue (MB). Based on the reduction current of MB, this electrochemical DNA sensor was able to detect the target ssDNA sequence of *hly* gene with a wide linear concentration range (1.0×10^{-14} to 1.0×10^{-6} mol L⁻¹) and a low detection limit (3.3×10^{-15} mol L⁻¹, 3σ). Furthermore, this biosensor was used to the detection of PCR amplification sample of *Listeria monocytogenes*.

Keywords: three-dimensional graphene, dendritic gold, electrochemical deposition, methylene blue, electrochemical DNA sensor.

1. INTRODUCTION

Graphene (GR) is a one-atom-thick planar carbon nanosheet with the properties such as large surface-to-volume ratio, tunable band gap, good electronic and thermal stability [1]. However GR is prone to form agglomerates due to strong planar stacking with π - π interaction, which limits its real applications. Compared with GR nanosheets, three-dimensional graphene (3DGR) exhibits the performance such as porous structure, fast mass transfer speed, high conductivity, network interconnection, effectively active surface, large loading capacity and mass transport kinetics [2].

Therefore the development of 3DGR can offer many usages in the fabrication of electrochemical devices [3]. Wang *et al.* summarized the synthesis and application of 3DGR in electrochemical sensor [4]. Various approaches including self-assembly, template-guided approaches, sol-gel, lightscribe patterning *etc.* have been devised for the preparations of 3DGR-related composites [5, 6]. 3DGR and its derivatives have various applications in electrochemistry and electrochemical sensor. Shi *et al.* obtained 3DGR by electro-reduction of graphene oxide (GO) for protein biosensor [7]. Sun *et al.* used solvent thermal reduction GO dispersion solution to synthesize a 3D structure rGO gel with high electrical conductivity, which was used for the fabrication of supercapacitors [8]. Sun *et al.* researched the electrochemistry of hemoglobin with 3DGR based electrode [9].

DNA sensor is a commonly used analytical tool for the analysis of specific target ssDNA sequence based on hybridization with complementary ssDNA sequence and recording the changes of responses. By using electrochemical method as the detection procedure, electrochemical DNA sensors have attracted attentions with the advantages of cheap instruments, rapid turnout, good selectivity [10, 11]. The usage of nanomaterials in the electrochemical DNA sensor can greatly enhance the sensitivity and selectivity. The presence of nanomaterials on electrode is suitable for probe ssDNA sequence immobilization and signal amplification. A DNA sensor with GR modified electrode was constructed by Wang *et al.* [12]. Liu *et al.* fabricated a sandwich-type DNA sensor with electrochemical co-reduced GR-three dimensional nanostructure gold nanocomposite [13]. Huang *et al.* fabricated a GR based electrochemical DNA sensor with low detection limit and wide detection range [14]. Gold nanomaterial is commonly used in electrochemistry with the properties including high conductivity, good biocompatibility and large surface area [15]. Zahra *et al.* fabricated a gold nanorods based electrochemical DNA sensor for hepatitis B virus [16].

In this paper, an electrochemical DNA sensor was fabricated by using 3DGR and nanosized gold modified electrode as the substrate electrode, which provided a porous interface with high conductivity. Mercaptoacetic acid (MAA) was self-assembled on Au/3DGR/CILE due to the specific binding of Au-S bond with the further covalently linked of the probe ssDNA sequences. This electrochemical DNA sensor demonstrated good performances on detection range, sensitivity, response time and stability.

2. EXPERIMENTAL

2.1. Apparatus

Voltammetric experiments were performed with CHI 750B electrochemical analyzer (Shanghai Chenhua Instrument, China) A three-electrode cell with the modified electrode as working electrode, saturated calomel electrode (SCE) as reference electrode and platinum wire electrode as auxiliary electrode was used. JSM-7100F scanning electron microscopy (SEM, Japan Electron Company, Japan) was recorded the morphologies. DNA extraction kit (Beijing

Tianguen Biotechnology Ltd. Co, China) was used and Eppendorf Mastercycler Gradient Polymerase Chain Reaction (PCR) system (Eppendorf, Germany) was chosen for amplification.

2.2. Reagents

1-Hexylpyridinium hexafluorophosphate (>99%, Lanzhou Yulu Fine Chemical Ltd. Co., China), graphite powder (Shanghai Colloid Chem. Plant, particle size of 30 μm), GO (Taiyuan Tanmei Co., China), lithium perchlorate (LiClO_4 , Chengdu Kelong Chem. Factory, China), HAuCl_4 (Tianjin Kaima Biochem. Ltd. Co., China), MAA (Shanghai Macklin Biochem. Ltd. Co., China), N-(3-dimethylamino-propyl)-N'-ethylcarbodiimide hydrochloride (EDC, Shanghai Macklin Biochem. Ltd. Co., China), N-hydroxy-succinimide (NHS, Shanghai Medpep Ltd. Co., China) and methylene blue (MB, Shanghai Chem. Plant, China) were used. TE buffer solution was prepared by 1.0 mmol L^{-1} pH 8.0 Tris-HCl buffer and 0.5 mmol L^{-1} pH 8.0 EDTA solution. The electrode activation solution was composed of 5.0 mmol L^{-1} EDC and 8.0 mmol L^{-1} NHS in 20 mmol L^{-1} pH 7.0 PBS solution. Doubly distilled water was used throughout and other chemicals were of analytical grade.

All the synthetic *hly* gene sequence related to *Listeria monocytogenes* were purchased from Shanghai Sangon Biological Engineering Tech. Ltd. Co. (China) as follows:

Probe ssDNA sequence: 5'-NH₂-TGG CGG CAC ATT TGT CAC TGC A-3',

Target ssDNA sequence: 5'-TGC AGT GAC AAA TGT GCC-GCC A-3',

One-base mismatched ssDNA sequence: 5'-TGC AGT GAC AGA TGT GCC GCC A-3',

Three-base mismatched ssDNA sequence: 5'-TGT AGT GAC AGA TGT GCA GCC A-3',

Non-complementary ssDNA sequence: 5'-CAT GTA CGT TGC GCC AAG TAG T-3'.

The sample for PCR reaction was got from frozen fish meat. The oligonucleotide primers for *hly* gene of *Listeria monocytogenes* were used as follows:

Primer F: 5'-AGG ATG CAT CTG CAT TCA A-3',

Primer R: 5'-GGA TAT CTG CAT TAT TTT GAT T-3'.

2.3. Fabrication of electrochemical DNA sensor

Carbon ionic liquid electrode (CILE) was acted as the substrate electrode and smoothed on weighing paper before use [17]. Then it was immersed in 3.0 mg mL^{-1} GO and 0.1 mol L^{-1} LiClO_4 solution with electrochemical deposition at constant potential (-1.3 V) for 50 s to obtain 3DGR/CILE. After drying 3DGR/CILE was put in a 5.0 mmol L^{-1} HAuCl_4 and 0.5 mol L^{-1} KNO_3 solution with electrodeposition carried out at constant potential (-0.4 V) for 300 s to get Au/3DGR/CILE, which was soaked in a 10.0 mmol L^{-1} MAA solution for 24 h for self-assembly. Then MAA/Au/3DGR/CILE was permeated in the electrode active solution for 30 min to active the electrode surface. Lastly 10.0 μL probe ssDNA solution (1.0×10^{-6} mol L^{-1} in pH 8.0 TE buffer) was dropped on MAA/Au/3DGR/CILE and dried at room temperature to get ssDNA/MAA/Au/3DGR/CILE. The amide reaction of carboxyl of MAA and the amino of probe ssDNA resulted in a stable immobilization of probe ssDNA sequence on the electrode. Afterwards the electrode was washed by 0.5% sodium dodecyl sulfate (SDS) solution and water three times to clear the surface.

2.4. Hybridization and electrochemical detection

DNA hybridization was implemented by dropping 8.0 μL target ssDNA sequence (in pH 8.0 TE buffer) on ssDNA/MAA/Au/3DGR/CILE at room temperature. After dried the electrode was flushed by 0.5% SDS solution and water in turn to wash the non-hybridized target DNA sequence. The resulted dsDNA/MAA/Au/3DGR/CILE was incubated in a 5.0×10^{-5} mol L^{-1} MB solution (in pH 7.0 PBS) for 10 min. Subsequently, the electrode was taken out and the electrochemical detection was performed in pH 7.0 PBS with DPV reduction peak current of MB as electrochemical signal. The instrumental parameters were set as follows: initial potential 0.2 V, final potential -0.7 V, pulse width 0.05 s, pulse amplitudes 0.05 V and sample width 0.0167 s.

2.5. PCR amplification

The unfrozen fish meat were cut to tiny pieces, placed in 10 mL peptone sorbit bile broth for the enrichment, and then incubated at 25 °C for 48 h to get the *Listeria monocytogenes* samples. The digest solution was then centrifuged at $12,000 \times g$ for 4 min. The pellet got after centrifugation was re-dissolved in 100 μL water and DNA was extracted by DNA extraction kit. Amplification of *hly* gene was performed in a final volume of 25 μL in 0.2 mL tube with 200.0 nmol L^{-1} each primer of *hly* gene sequence, $10 \times$ reaction buffer B, 2.0 mmol L^{-1} MgCl_2 , 200.0 nmol L^{-1} each of dATP, dCTP, dGTP and dTTP, 1.5 units of Taq DNA polymerase and 1.0 μL DNA template purified from samples. In PCR procedure DNA was initially denatured at 94 °C for 30 s. PCR conditions were set with following procedure, 35 cycles of amplification (94 °C for 30s, 56 °C for 30 s, 72 °C for 30 s) and extension at 72 °C for 5 min. 6 μL PCR product was analyzed by electrophoresis separation (5 V cm^{-1} , 40 min) by using a 2% agarose gel with 0.5 $\mu\text{g mL}^{-1}$ of ethidium bromide in $1 \times$ TAE buffer. The final products were put into refrigerator for storage.

3. RESULTS AND DISCUSSION

3.1. SEM of the materials

The morphology of the electrodeposited 3DGR and dendritic Au nanomaterial were observed by SEM. 3DGR with different magnitude was illustrated in Fig. 1 A and B, which showed a porous structure with scrolled sheet and large lamellate [18, 19]. Then Au was electrodeposited with dendritic appearance grown on 3DGR/CILE (Fig. 1 C and D). The presence of dendritic Au nanomaterials on the electrode further increased the surface area and accelerated the electron transfer rate with the electrochemical response amplified.

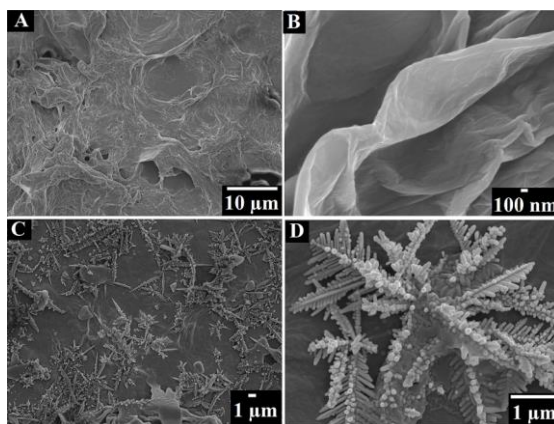


Figure 1. SEM images of 3DGR with different magnitude on CILE (A, B) and dendritic Au nanomaterials on the surface of 3DGR (C, D).

3.2. Electrochemical characteristics of the modified electrodes

Cyclic voltammograms of different electrodes in a $K_3[Fe(CN)_6]$ and KCl solution were shown in Fig. 2. The biggest redox currents appeared on Au/3DGR/CILE (curve e), showing the highest conductivity of Au/3DGR nanocomposite. The redox currents decreased gradually on MAA/Au/3DGR/CILE (curve d), ssDNA/MAA/Au/3DGR/CILE (curve c), dsDNA/MAA/Au/3DGR/CILE (curve b) and CILE (curve a), which was due to the presence of negatively charged DNA and MAA hindered the diffusion of negative charged $[Fe(CN)_6]^{3-/4-}$ to electrode [20]. The effective surface area (A) of Au/3DGR/CILE was calculated with different scan rates by employing the Randles-Servick equation [$I_{pc}=(2.69 \times 10^5)n^{3/2}AD^{1/2}C^*v^{1/2}$] [21] and the value was 1.23 cm^2 , 5 times larger than that of CILE. Therefore 3DGR with large surface area could act as a platform for the loading of Au nanomaterials, which enabled more probe ssDNA immobilized on the modified electrode.

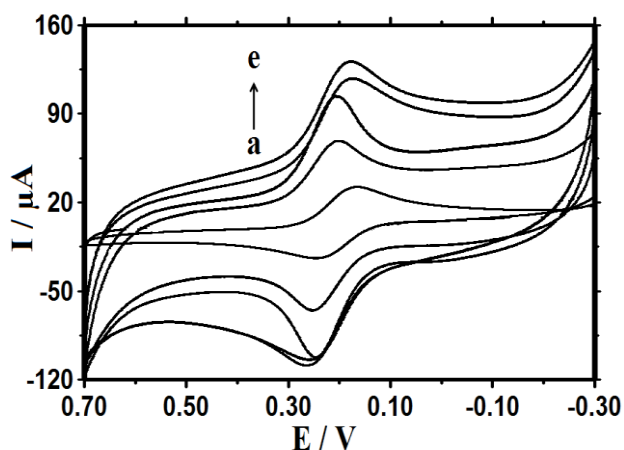


Figure 2. Cyclic voltammograms of various electrodes in a $1.0 \text{ mmol L}^{-1} K_3[Fe(CN)_6]$ and $0.5 \text{ mol L}^{-1} KCl$ solution with scan rate as 100 mV s^{-1} . Electrodes: (a) CILE, (b) dsDNA/MAA/Au/3DGR/CILE, (c) ssDNA/MAA/Au/3DGR/CILE, (d) MAA/Au/3DGR/CILE and (e) Au/3DGR/CILE.

3.3. Electrochemical behaviors of MB on different DNA modified electrodes

As a frequently utilized electrochemical indicator for DNA sensor, MB can distinguish ssDNA or dsDNA with different model [22]. MB can interaction with the phosphoric acid skeleton of ssDNA by electrostatic adsorption. Also electrostatic attraction and/or intercalation with major or minor grooves of dsDNA are present [23, 24]. Fig. 3 illustrated the DPV peaks of MB after reacted with ssDNA and dsDNA based electrode. The reduction current of MB on dsDNA/MAA/Au/3DGR/CILE (curve d) was bigger than that of ssDNA/MAA/Au/3DGR/CILE (curve b), indicating dsDNA on the electrode had groove interaction with more MB molecules adsorbed. Similar results also appeared on dsDNA/MAA/Au/CILE (curve c) and ssDNA/MAA/Au/CILE (curve a). Also the reduction peak of MB on curve d was bigger than that of curve c, proving 3DGR on the electrode could provide a large surface area for the loading of more ssDNA sequences.

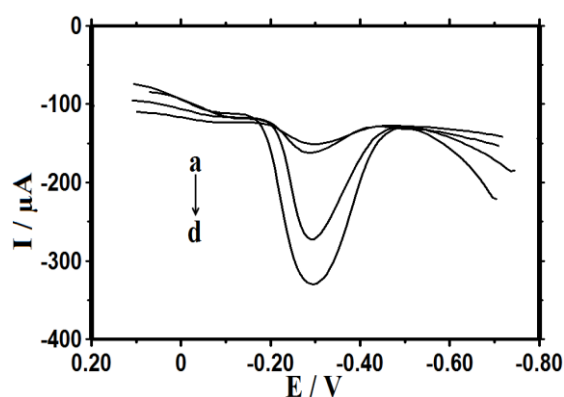


Figure 3. DPV of (a) ssDNA/MAA/Au/CILE; (b) ssDNA/MAA/Au/3DGR/ CILE; (c) dsDNA/MAA/Au/CILE; (d) dsDNA/MAA/Au/3DGR/CILE in a 20.0 mmol L⁻¹ pH 7.0 PBS buffer containing 5.0×10⁻⁵ mol L⁻¹ MB.

3.4. Selectivity

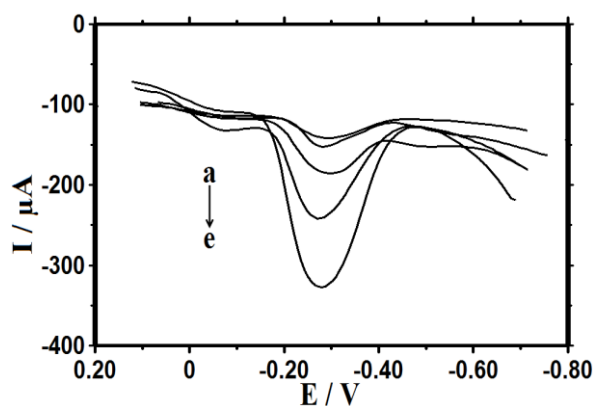


Figure 4. DPV of 20.0 mmol L^{-1} MB on the probe ssDNA modified electrode (a), hybridized with non-complementary (b), three-base mismatched (c), one-base mismatched (d) and complementary ssDNA sequence (e).

The selectivity was tested with DPV after hybridization with different ssDNA sequence. As shown in Fig. 4, voltammetric current of MB on probe ssDNA modified electrode (curve a) was the lowest one. After hybridized with non-complementary (curve b), three-base mismatched ssDNA sequence (curve c), one-base mismatched ssDNA sequence (curve d) and complementary ssDNA sequence (curve e), the reduction peak current increased gradually, which indicated that the formation of dsDNA molecules on the electrode was benefit for accumulating more MB on the electrode surface [25]. Therefore the responses increased gradually on different electrodes.

3.5. Working curve

The fabricated electrochemical DNA biosensor was used to hybridize with different concentrations of complementary target ssDNA. As shown in Fig. 5, the DPV signals increased gradually with increasing of target ssDNA concentrations, showing a gradually formation of dsDNA on the electrode surface that could accumulate more MB molecules with the electrochemical responses increased gradually. A well linear relationship of the current and the logarithm of concentration was got from 1.0×10^{-14} to $1.0 \times 10^{-6} \text{ mol L}^{-1}$ with a detection limit of $3.3 \times 10^{-15} \text{ mol L}^{-1}$ (3σ). As shown in inset of Fig. 5, the linear regression equation was $\Delta I (\mu\text{A}) = -21.71 \log[C/(\text{mol L}^{-1})] - 337.90$ ($\gamma=0.996$). In compare to some electrochemical DNA biosensors that listed in table 1, this developed DNA sensor had the lower detection limit and the wider linear range for complementary target ssDNA sequences.

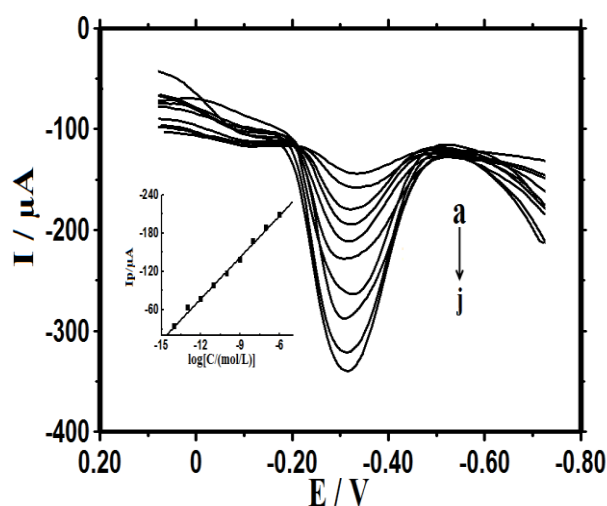


Figure 5. DPV of MB on probe ssDNA modified electrode after hybridization with different concentrations of target ssDNA sequence. Concentrations from a to j were 0, 1.0×10^{-14} , 1.0×10^{-13} , 1.0×10^{-12} , 1.0×10^{-11} , 1.0×10^{-10} , 1.0×10^{-9} , 1.0×10^{-8} , 1.0×10^{-7} and $1.0 \times 10^{-6} \text{ mol L}^{-1}$, respectively. Insert: plots of ΔI versus $\log C$.

3.6. Stability and reproducibility

Stability was obtained by storing the modified electrode for 10 days and then used for hybridized with target ssDNA, which remained 96.1% of the starting value. This result indicated the proposed DNA sensor exhibited excellent stability. The relative standard deviation (RSD) of probe ssDNA modified electrode hybridized with target ssDNA sequence for 7 repeated detections was 3.3%, indicating a satisfactory reproducibility.

Table 1. Comparison of analytical parameters of the electrochemical DNA sensors.

Modified electrodes	Detection technique	Linear range (M)	Detection limit (M)	Reference
GNRs/AuE	DPV	1.0×10^{-12} to 1.0×10^{-5}	2.0×10^{-12}	26
AuNPs/rGO/GCE	DPV	1.0×10^{-13} to 1.0×10^{-8}	3.5×10^{-14}	27
Ph-NH ₂ /GO/GCE	EIS	1.0×10^{-12} to 1.0×10^{-7}	1.1×10^{-13}	28
rGO/GR	EIS	1.0×10^{-12} to 1.0×10^{-7}	1.58×10^{-13}	29
WS ₂ -GR/GCE	DPV	1.0×10^{-14} to 5.0×10^{-10}	2.3×10^{-15}	30
ECR/GCE	DPV	5.0×10^{-12} to 2.0×10^{-10}	9.8×10^{-11}	31
Au/3DGR/CILE	DPV	1.0×10^{-14} to 1.0×10^{-6}	3.3×10^{-15}	This work

GNRs: gold nanorods; AuE: Au electrode; Au NPs: gold nanoparticles; rGO: reduced graphene oxide; GCE: glassy carbon electrode; Ph-NH₂: *p*-Phenylenediamine; GO: graphene oxide; WS₂: tungsten sulfide; ECR: eriochrome cyanine R

3.7. PCR products of Detection

To verify the practicability of the proposed electrochemical DNA sensor, the PCR amplification sample was detected, which was diluted for 10 times in a 50 mmol L⁻¹ pH 8.0 TE buffer, heated in boiling water for 10 min and cooled in ice water bath for 2 min to get ssDNA sequence. Then the solution was employed to hybridize with probe ssDNA on the modified electrode, and the signal of MB was recorded by DPV technique with the curves present in Fig. 6. The MB reduction currents on MAA/Au/3DGR/CILE (curve a), ssDNA/MAA/Au/3DGR/CILE (curve b) and the electrode of hybridized with PCR product (curve c) increased greatly. The result showed that the PCR product could hybridize with the probe ssDNA sequence on the electrode with dsDNA formed, which accumulated more MB on the electrode with the current increased greatly [32].

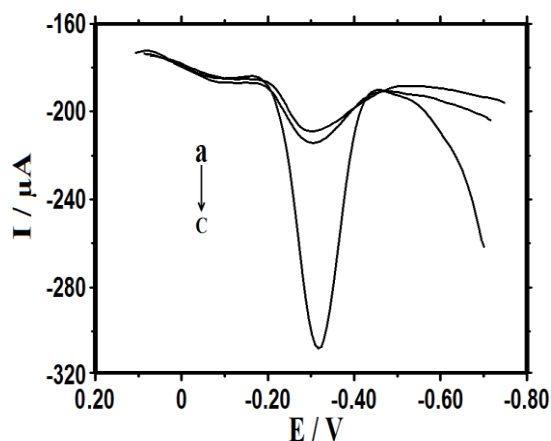


Figure 6. DPV of MB on MAA/Au/3DGR/CILE (a), ssDNA/MAA/Au/3DGR/CILE (b) and hybridized with PCR sample of *Listeria monocytogenes* (c).

4. CONCLUSION

In summary three-dimensional GR and dendritic nano-Au modified CILE was acted as the substrate electrode. Then NH_2 -modified probe ssDNA sequence could be covalently linked Au/3DGR/CILE with the help of MAA, EDC and NHS. Voltammetry was employed to investigate the performances of different modified electrodes. The proposed electrochemical DNA sensor was applied to identify the target ssDNA sequence of *hly* gene related to *Listeria monocytogenes* with the advantages including good selectivity, stability and reproducibility, low detection limit and wide linear range.

ACKNOWLEDGEMENTS

We acknowledge the financial support of the International Science and Technology Cooperation Project of Hainan Province (KJHZ2015-13), the Program for Innovative Research Team in University (IRT-16R19) and Graduate Student Innovation Research Project of Hainan Province (Hys2016-61).

References

1. D. Chen, H. Feng and J. Li, *Chem. Rev.*, 112 (2012) 6027.
2. S. Han, D. Wu, S. Li, F. Zhang and X. Feng, *Adv. Mater.*, 26 (2016) 849.
3. J. Liu, T. Wang, J. Wang and E. Wang, *Electrochim. Acta*, 161 (2015) 17.
4. H. Wang, X. Z. Yuan, G. M. Zeng, Y. Wu, Y. Liu, Q. Jiang and S. S. Gu, *Adv. Colloid Interface Sci.*, 221 (2015) 41.
5. C. Li and G. Shi, *Nanoscale*, 4 (2012) 5549.
6. J. Zhang, F. Zhao, Z. Zhang, N. Chen and L. Qu. *Nanoscale*, 5 (2013) 3112.
7. F. Shi, J. W. Xi, F. Hou, L. Han, G. J. Li, S. X. Gong, C. X. Chen and W. Sun, *Mater. Sci. Eng. C-Mater.*, 58 (2016) 450.
8. Y. Q. Sun, Q. Wu and G. Q. Shi, *Phys Chem. Chem. Phys.*, 13 (2011) 17249.
9. W. Sun, F. Hou, S. X. Gong, L. Han, W. C. Wang, F. Shi, J. W. Xi, X. L. Wang and G. J. Li, *Sensor. Actuat. B-Chem.*, 219 (2015) 331.
10. L. Wang, Q. Zhang, S. Chen, F. Xu, S. Chen, J. Jia, H. Tan, H. Hou and Y. Song, *Anal. Chem.*, 86 (2014) 1414.
11. X. W. Han, X. Fang, A. Q. Shi, J. Wang and Y. Z. Zhang, *Anal. Biochem.*, 443 (2013) 117.

12. L. Wang, E. H. Hua, M. Liang, C. X. Ma, Z. L. Liu, S. C. Sheng, M. Liu, G. M. Xie and W. L. Feng, *Biosens. Bioelectron.*, 51 (2014) 201.
13. A. L. Liu, G. X. Zhong, J. Y. Chen, S. H. Weng, H. N. Huang, W. Chen, L. Q. Lin, Y. Lei, F. H. Fu, J. H. Lin and S. Y. Yang, *Anal. Chim. Acta*, 767 (2013) 50.
14. K. J. Huang, Y. J. Liu, H. B. Wang, T. Gan, Y. M. Liu and L. L. Wang, *Sensor. Actuat. B-Chem.*, 191 (2014) 828.
15. M. Vidotti, R. F. Carvalhal and R. L. Mendes, *J. Braz. Chem. Soc.*, 22 (2011) 3.
16. Z. Shakoori, S. Salimian, S. K. Mahdi Adabi and R. Saber, *Anal. Bioanal. Chem.*, 407 (2015) 455.
17. X.L. Niu, L.J. Yan, X.B. Li, A.H. Hu, C.J. Zheng, Y.L. Zhang and W. Sun, *Int. J. Electrochem. Sci.*, 11 (2016) 1720.
18. K. X. Sheng, Y. Q. Sun, C. Li, W. J. Yuan and G.Q. Shi, *Sci. Rep.*, 2 (2012) 247.
19. H. L. Sha, W. Zheng, F. Shi, X. F. Wang and W. Sun, *Int. J. Electrochem. Sci.*, 11 (2016) 9656.
20. W. Sun, M. X. Yang, J. H. Zhong and K. Jiao, *Acta Phys.-Chim. Sin.*, 23 (2007) 499.
21. A. J. Bard and L. R. Faulkner, *Electrochemical methods: fundamentals and applications*. Wiley, New York, 2001.
22. P. Kara, K. Kerman and D. Ozkan, *Electrochem. Commun.*, 4 (2002) 705.
23. D. Pan, X. L. Zuo, Y. Wan, L. H. Wang, J. Zhang, S. P. Song and C. H. Fan, *Sensors*, 7 (2007) 2671.
24. W. Yang, M. Ozsonz, D. B. Hibbert and J. J. Gooding, *Electroanalysis*, 14 (2002) 1299.
25. W. Sun, P. Qin, H. W. Gao, G. C. Li and K. Jiao, *Biosens. Bioelectron.*, 25 (2010) 1264.
26. A. Shakoori, S. Salimian, S. Kharrazi, M. Adabi and R. Saber, *Anal. Bioanal. Chem.*, 407 (2015) 455.
27. Y. Z. Zhang and W. Jiang, *Electrochim. Acta*, 71 (2012) 239.
28. Y. W. Hu, F. H. Li, D. X. Han, T. S. Wu, Q. X. Zhang, L. Niu and Y. Bao, *Anal. Chim. Acta*, 753 (2012) 82.
29. B. Li, G. H. Pan, N. D. Avent, R. B. Lowry, T. E. Madgett and P. L. Wainnes, *Biosens. Bioelectron.*, 72 (2015) 313.
30. K. J. Huang, Y. J. Liu, H. B. Wang, T. Gan, Y. M. Liu and L. L. Wang, *Sensor. Actuat. B-Chem.*, 443 (2013) 117.
31. L. Wang, L. Q. Lin, X. W. Xu, S. H. Weng, Y. Lei, A. L. Liu, Y. Z. Chen and X. H. Lin, *Electrochim. Acta*, 69 (2012) 56.
32. W. Sun, X. L. Qi, Y. Y. Zhang, H. R. Yang, H. W. Gao, Y. Chen and Z. F. Sun, *Electrochim. Acta*, 85 (2012) 145.